Article

A DFT Study on the Formation of a Phosphohistidine Intermediate in Prostatic Acid Phosphatase

Satyan Sharma, Arvi Rauk, and Andre# H. Juffer

J. Am. Chem. Soc., **2008**, 130 (30), 9708-9716 • DOI: 10.1021/ja710047a • Publication Date (Web): 08 July 2008

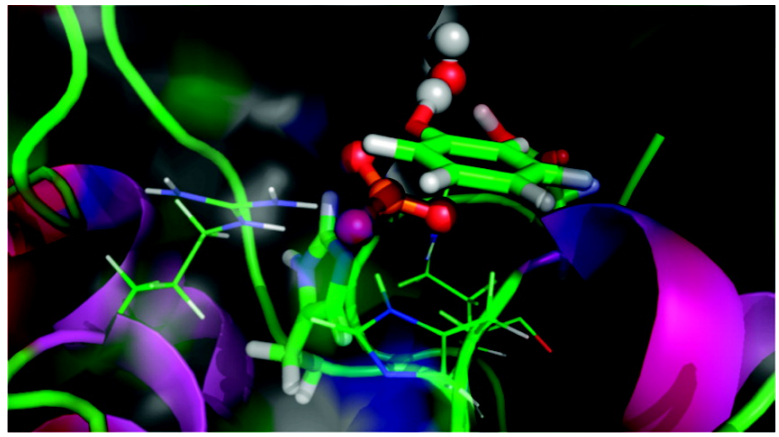

J|A|C|S
ARTICLES

Published on Web 07/08/2008

A DFT Study on the Formation of a Phosphohistidine Intermediate in Prostatic Acid Phosphatase

Satyan Sharma,[†] Arvi Rauk,[‡] and André H. Juffer*,[†]

Biocenter Oulu and the Department of Biochemistry, University of Oulu, Oulu, Finland and Department of Chemistry, University of Calgary, 2500 University Drive NW, Calgary, AB, Canada T2N 1N4

Received November 6, 2007; E-mail: andre.juffer@oulu.fi

Abstract: Histidine phosphatases are a class of enzymes that are characterized by the presence of a conserved RHGXRXP motif. This motif contains a catalytic histidine that is being phosphorylated in the course of a dephosphorylation reaction catalyzed by these enzymes. Prostatic acid phosphatase (PAP) is one such enzyme. The dephosphorylation of phosphotyrosine by PAP is a two-step process. The first step involves the transfer of a phosphate group from the substrate to the histidine (His12). The present study reports on the details of the first step of this reaction, which was investigated using a series of quantum chemistry calculations. A number of quantum models were constructed containing various residues that were thought to play a role in the mechanism. In all these models, the transition state displayed an associative character. The transition state is stabilized by three active site arginines (Arg11, Arg15, and Arg79), two of which belong to the aforementioned conserved motif. The work also demonstrated that His12 could act as a nucleophile. The enzyme is further characterized by a His257-Asp258 motif. The role of Asp258 has been elusive. In this work, we propose that Asp258 acts as a proton donor which becomes protonated when the substrate enters the binding pocket. Evidence is also obtained that the transfer of a proton from Asp258 to the leaving group is possibly mediated by a water molecule in the active site. The work also underlines the importance of His257 in lowering the energy barrier for the nucleophilic attack.

1. Introduction

Phosphates are involved in many biological processes, such as the hydrolysis of ATP which is relevant for the energy household of cells, the degradation of nucleoside guanosine, the regulation of oxidative phosphorylation, the regulation of starch synthesis, the synthesis of fatty acids, and numerous cell signaling processes.[1] Consequently, reactions involving phosphates have long been investigated by both experimental and theoretical approaches.[2,3] Specifically, a number of enzymes that catalyze phosphorylation and dephosphorylation reactions have been extensively studied with an effort to understand their mechanism to broaden the understanding of these chemical processes and to identify more efficient drugs.

Prostatic acid phosphatase (PAP, EC 3.1.3.2) is one such enzyme. It is capable of (de)phosphorylating tyrosine residues. The enzyme can be found in high amounts in the serum of subjects with prostatic carcinoma[4] and has been used as one of the biochemical markers in staging prostatic cancer.[5] Lin et al.[6] observed a negative correlation between cellular levels of PAP and the growth of various human prostate cancer cell lines. It has been suggested that PAP could be involved in regulating prostate cell growth by dephosphorylating activated growth receptors in the cell membrane. These receptors are phosphorylated upon binding of their respective ligands (growth hormones) resulting in signal transmission across the cell membrane, stimulating the growth of the cell. Dephosphorylation of these receptors attenuates the signaling process. It has been shown earlier that PAP could bind to phosphorylated growth receptors such as the Epidermal Growth Factor Receptor (EGFR) and its homologue (Erbb-2) and could affect their dephosphorylation state.[7,8] In our previous study on PAP, we have shown that the enzyme could bind to phosphorylated tyrosine-containing peptides derived from these receptors, using pK_a (acid dissociation constant) calculations, ligand docking, and molecular dynamics (MD) simulations.[9]

Dephosphorylation reactions in nonmetalloenzymes require a phosphotransfer step. The transition state could occur anywhere between two extremes, the dissociative and associative state. In a dissociative mechanism, there is a complete bond cleavage to the leaving group with no appreciable bond formation to the nucleophile. In an associative mechanism, the nucleophile and leaving group are both bonded in a pentaco-

[†] University of Oulu.
[‡] University of Calgary.

(1) Horton, H. R.; Moran, L. A.; Scrimgeour, K. G.; Perry, M. D.; Rawn, J. D. *Principles of biochemistry*; Pearson Prentice Hall: New York, 2006.
(2) Martin, B. L.; Graves, D. J. *J. Biol. Chem.* **1986**, *261*, 14545–14550.
(3) Kolmodin, K.; Aqvist, J. *FEBS Lett.* **2001**, *498*, 208–213.
(4) Gutman, E. B.; Sproul, E. E.; Gutman, A. B. *Am. J. Cancer* **1936**, *28*, 485–495.
(5) Lin, M. F.; DaVolio, J.; Garcia-Arenas, R. *Cancer Res.* **1992**, *52*, 4600–4607.
(6) Lin, M. F.; Lee, M. S.; Zhou, X. W.; Andressen, J. C.; Meng, T. C.; Johansson, S. L.; West, W. W.; Taylor, R. J.; Anderson, J. R.; Lin, F. F. *J. Urol.* **2001**, *166*, 1943–1950.
(7) Lin, M. F.; Clinton, G. M. *Mol. Cell. Biol.* **1988**, *8*, 5477–5485.
(8) Meng, T. C.; Lin, M. F. *J. Biol. Chem.* **1998**, *273*, 22096–22104.
(9) Sharma, S.; Pirila, P.; Kaija, P. H.; Vihko, P.; Juffer, A. H. *Proteins* **2005**, *58*, 295–308.

 10.1021/ja710047a CCC: $40.75

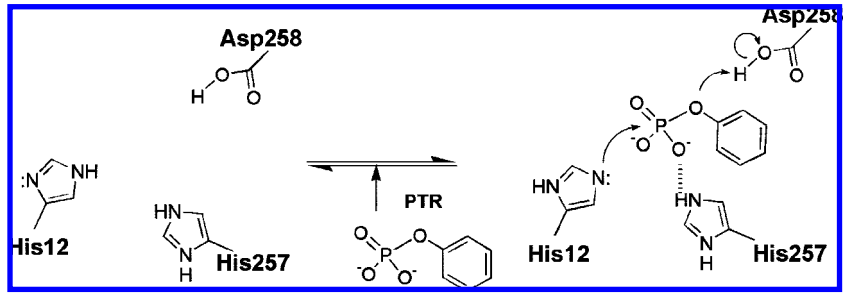

Figure 1. First step of the reaction mechanism of PAP. His12 acts as the attacking nucleophile. With the formation of the phosphohistidine intermediate, the substrate (PTR) is released as phenol. Asp258 acts as the general base in the enzyme active site.

ordinated intermediate. Studies on protein tyrosine phosphatases (PTPases) have shown that the reaction proceeds through a dissociative mechanism in these enzymes.[3,10] The well studied PTPases rely on an active Cys as a nucleophile. These enzymes catalyze the reaction in a two-step process, an initial formation of an phosphoenzyme intermediate followed by the hydrolysis of the intermediate, with the involvement of a nearby Asp, so as to regenerate the enzyme.[11,12] There is a general agreement that PAP also catalyzes dephosphorylation via a similar two-step process. The enzyme has conserved residues 11−17, the RHGXRXP motif,[13] of which the histidine acts as a nucleophile.[12,14,15] The nucleophilic attack results in the formation of a phosphohistidine intermediate which in the next step is hydrolyzed to regenerate the enzyme. The reaction mechanism for PAP shown in Figure 1 is adopted from the mechanism originally proposed for fructose-2,6-bisphosphatase.[16] The scheme identifies His12 as the nucleophilic attacking group and Asp258 as the general acid. The conserved His257-Asp258 combination is commonly referred to as the His-Asp motif.[17] His257 (Figure 1) has been proposed to be important for substrate binding.[12,18]

There is no clear understanding on the details of the mechanism of the first step. The literature lacks any mechanistic studies on the histidine phosphatases, or any enzyme using histidine as a nucleophile in general. Some authors, based on the crystal structure and other experimental studies, suggested that the proton to the leaving group is donated by the active site Asp (Asp258).[18,19] Others,[20] based on their crystal structure of liganded human PAP, suggested that the Asp258 cannot act as a general acid, because (*i*) it is too far away from the ligand and (*ii*) it is in close proximity to Arg15 and thus would remain unprotonated. In our previous study,[9] we proposed that in the free enzyme Asp258 remains unprotonated. In the same study we reported that there is a strong upward shift of the pK_a of Asp258 when a highly negative ligand enters the binding pocket. Thus, the ligand enters the binding site as a monoanion ($ROPO_3H^-$) as dictated by the pK_a's of the phosphate group free in solution, but it immediately donates its proton to Asp258 to become a dianion ($ROPO_3^{2-}$).

To validate this proposal and to further foster the understanding of the reaction mechanism of PAP, a series of quantum mechanical (QM) calculations on the first step of the reaction have been carried out, with phenylphosphate (PTR, as a model for phosphorylated tyrosine) as the substrate. To determine the nature of phosphoryl transfer between phenylphosphate and imidazole of His12, the energy barriers in the gas phase, in solvent, and in the protein environment were analyzed in detail. This work presents for the first time, to the best of our knowledge, the mechanism of intermediate formation in a histidine phosphatase and also provides evidence for a possible involvement of catalytic water in the reaction. The enzyme also serves as a model system for other histidine phosphatases.

2. Materials and Method

All QM calculations were carried out with the Gaussian 98[21] and Gaussian 03[22] suite of programs. Geometry optimizations for models I to VI were performed using the B3LYP hybrid density functional theory (DFT) methods with the 6-31+G(d) basis set. To obtain more accurate energies, single-point calculations were performed with 6-311+G(2df, p), unless stated otherwise. Harmonic frequency analysis of each structure was carried out at B3LYP/6-31+G(d) to confirm stationary points. For two-layer ONIOM (which stands for "our own N-layered integrated molecular orbital combined with molecular mechanics")[23–25] calculations all the atoms (including waters) within a 15 Å sphere around the phosphate atom of the ligand were included. Only the atoms within 12 Å of the P atom were allowed to optimize, and the rest were fixed to their respective coordinates. The B3LYP/6-31G(d) basis set was employed for the QM region, which has been successful in locating intermediates on the potential energy surface.[26,27] The rest of the atoms were described with AMBER force field parameters. The covalent bonds at the boundary between the two regions were treated using a link-atom approach as implemented in Gaussian

(10) Zhang, Z. Y. *Crit. Rev. Biochem. Mol. Biol.* **1998**, *33*, 1–52.
(11) Zhang, Z.; Harms, E.; Van Etten, R. L. *J. Biol. Chem.* **1994**, *269*, 25947–25950.
(12) Ostanin, K.; Saeed, A.; Van Etten, R. L. *J. Biol. Chem.* **1994**, *269*, 8971–8978.
(13) Van Etten, R. L.; Davidson, R.; Stevis, P. E.; MacArthur, H.; Moore, D. L. *J. Biol. Chem.* **1991**, *266*, 2313–2319.
(14) Van Etten, R. L. *Ann. N.Y. Acad. Sci.* **1982**, *390*, 27–51.
(15) Ostanin, K.; Harms, E. H.; Stevis, P. E.; Kuciel, R.; Zhou, M. M.; Van Etten, R. L. *J. Biol. Chem.* **1992**, *267*, 22830–22836.
(16) Okar, D. A.; Live, D. H.; Devany, M. H.; Lange, A. J. *Biochemistry* **2000**, *39*, 9754–9762.
(17) Kerovuo, J.; Rouvinen, J.; Hatzack, F. *Biochem. J.* **2000**, *352*, 623–628.
(18) Porvari, K. S.; Herrala, A. M.; Kurkela, R. M.; Taavitsainen, P. A.; Lindqvist, Y.; G.; Schneider, G.; Vihko, P. T. *J. Biol. Chem.* **1994**, *269*, 22642–22646.
(19) Zhang, X. Q.; Lee, M.-S.; Zelivianski, S.; Lin, M. F. *J. Biol. Chem.* **2001**, *276*, 2544–2550.
(20) Ortlund, E.; LaCount, M. W.; Lebioda, L. *Biochemistry* **2003**, *42*, 383–389.
(21) Frisch, M. J.; et al. *Gaussian 98*, revision A.11; Gaussian, Inc.: Pittsburgh, PA, 1998.
(22) Frisch, M. J.; et al. *Gaussian 03*, revision C.02; Gaussian, Inc.: Wallingford, CT, 2004.
(23) Humbel, S.; Sieber, S.; Morokuma, K. *J. Chem. Phy.* **1996**, *105*, 1959–1967.
(24) Svensson, M.; Humbel, S.; Froese, R. D. J.; Matsubara, T.; Sieber, S.; Morokuma, K. *J. Phys. Chem.* **1996**, *100*, 19357–19363.
(25) Froese, R. D. J.; Morokuma, K. In *Encyclopedia of Computational Chemistry*; Schleyer, P. v. R., Ed.; Wiley: New York, 1998; pp 1245−1247.

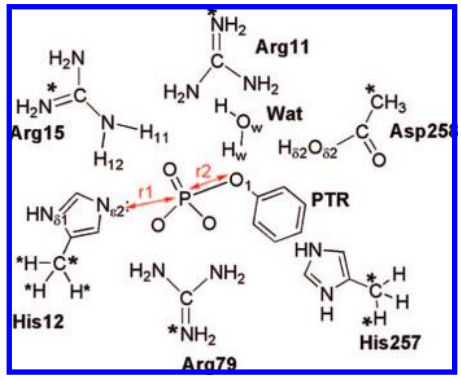

Figure 2. Schematic of the models used in this study. Model II contains Arg11+His12+Arg15+Arg79+PTR. Model III is similar but with frozen atoms. Frozen atoms are marked with an asterisk. Model IV includes Model III+His257. Model V and VI include an additional water (Wat). The reaction coordinates r1 and r2 are marked in red.

03. Further, single-point energy calculations were performed for the intermediates on the potential energy surface with B3LYP/6-31+G(d):AMBER to obtain better energies. Only the QM region was used to locate a fully optimized transition state using the 6-31+G(d) basis set.

All MD simulations were performed with GROMACS.[28,29] Note that, for the MD simulation, the His12 was protonated at the $N_{\varepsilon 2}$ position and not at the $N_{\delta 1}$ position. The backbone of the loops corresponding to the aminoacids 63−66 and 90−110 was position restrained during MD simulations. These loops show a bending motion when a monomer of the enzyme is simulated. The essential dynamics analysis confirmed that this motion could alter the properties of the binding site. To avoid the artifacts of simulating a monomer, which in fact is not observed in the case of a dimer, these regions were position restrianed during the simulations. The results along with further details of the simulation setup can be found elsewhere.[9] Structures of enzymes were obtained from the RCSB protein data bank (PDB).[30]

We used different model systems to investigate the details of the first step of the reaction catalyzed by PAP, each of which is described below. The various labels that were employed to identify atoms and chemical groups are explained in Figure 2.

2.1. Model I. This model consists of an imidazole (Im) and monoanionic phenylphosphate ($PheOPO_3H^-$) characterizing the basic chemical event occurring during the phosphoryl transfer. The reactants were optimized individually in the gas phase, and gaseous phase quantities were calculated. For transition state (TS) calculations, the input guess was modeled by placing the metaphosphate group HPO_3^- equidistant (1.90 Å) from the oxygen of phenolate and nucleophilic nitrogen of imidazole with the relative orientation of the phenyl and imidazole rings obtained from crystal structure 1ND5. To verify the transition state as real, the mapping of the energy surface near the found TS was also carried out. Single-point energies were calculated at the B3LYP/6-311+G(2df, 2p) level. The influence of solvation was investigated by repeating the calculation in the presence of a polarizable solvent modeled with the conductor-like polarizable continuum model (CPCM).[31−33] The solvent was modeled as water. The gaseous phase 0.001 electrons $bohr^3$ isodensity surface was used to define the solvent cavity.

2.2. Model II. Model II consists of imidazole, phenylphosphate, and three guanidium ions (to emulate the nearby Arg11, Arg15, and Arg79). The initial coordinates of the atoms in this model system were obtained from the X-ray crystallographic structure of PAP complexed with α-benzylaminobenzyl phosphonic acid (PDB entry 1ND5[20]). The ligand was replaced with a phosphotyrosine capped at N- and C-termini by an acyl (Ace) group and an amino (NH_2) group. The complex was subjected to a 1000 step steepest descent energy minimization using GROMACS. This was then used to construct Model II. This model was basically employed to evaluate the choice of reaction coordinates for subsequent calculations. The distance between the P atom of the ligand phosphotyrosine and the nucleophilic atom NE2 of His12 is referred to as r1, Figure 2. The distance between the bridging oxygen (O_1) and P of the ligand is referred to as r2. Using r1 and r2 as the two reaction coordinates, a relaxed Potential Energy Surface (PES) was constructed in the following way. The initial values of r1 and r2 were kept fixed at 3.40 and 1.75 Å. The choice of 3.4 Å is based on our previous molecular dynamics simulation results where it was shown that the average distance between the P of the ligand and the nucleophilic N of His12 was 3.42 Å.[9] Subsequently, several optimizations were carried out with varying values for r1 and r2. The coordinate r1 was changed from 3.40 to 1.75 Å in steps of 0.25 Å. Simultaneously, r2 was varied from 1.75 to 3.40 Å for every value of r1, with all other degrees of freedom free to optimize. The lowest point on the path connecting reactants and products was used as an initial guess for the transition state (TS) optimization, followed by a frequency calculation to verify the saddle point.

2.3. Model III. Model III is similar to Model II except the arginines (as guanidium ions) are now frozen at their respective N_ε positions. The His12 is modeled as methyl imidazole with the methyl group frozen. Asp258, modeled as acetate, is frozen at the methyl carbon. The atoms were frozen to mimic the active site geometry and are marked with an asterisk in Figure 2. The reactants and products were optimized in the same manner as that described for Model II (r1 = 3.40 Å, r2 = 1.75 Å to identify the reactants and r1 = 1.75 Å, r2 = 3.40 Å to identify the products). The TS obtained for Model II served as the guess structure for TS optimizations with Model III. As for Model II, the TS optimization was followed by a frequency calculation.

2.4. Model IV. This model is similar to Model III with His257 included. The starting geometries were obtained using the two-layer ONIOM methodology. The phenylphosphate and parts of the side chains of the amino acids Arg11, His12, Arg15, Arg79, His257, Asp258 were included in the QM motif. The distances $N_{\varepsilon 2}$−P (r1) and P−O_1 (r2) were fixed at 3.40 and 1.75 Å, respectively, to describe the reactants. To describe the products, r1 and r2 distance values were fixed at 1.75 and 3.40 Å, respectively. The initial structure for the TS optimization was obtained from Model II. After optimizing the ONIOM system, at putative stationary points, the QM subsystem was excised and used for higher level DFT calculations.

2.5. Model V. Model V includes an additional water in the QM part but is otherwise identical to Model IV. The position of water was obtained from a 5 ns long MD simulation. One of the structures observed in the simulation was arbitrarily chosen, was energy minimized, and served as a starting point for the subsequent ONIOM calculations, which were performed in a similar way as in the case of Model IV. A PES scan was carried out using the aforementioned reaction coordinates, to obtain a reasonable guess for the TS optimizations, as before.

2.6. Model VI. The last model contains neutral His257; the rest of the model is identical to Model V. The initial structures were obtained in a similar way as in the case of Model V. The MD simulation was redone (see Model V) for 2.5 ns, but now with a

(26) Cheng, Y.; Zhang, Y.; McCammon, J. A. *J. Am. Chem. Soc.* **2005**, *127*, 1553–1562.
(27) Alberts, I. L.; Wang, Y.; Schlick, T. *J. Am. Chem. Soc.* **2007**, *129*, 11100–11110.
(28) Berendsen, H. J. C.; van der Spoel, D.; van Drunen, R. *Comput. Phys. Commun.* **1995**, *91*, 43–56.
(29) Lindahl, E.; Hess, B.; van der Spoel, D. *J. Mol. Mod.* **2001**, *7*, 306–317.
(30) Berman, H. M.; Westbrook, J.; Feng, Z.; Gilliland, G.; Bhat, T. N.; Weissig, H.; Shindyalov, I. N.; Bourne, P. E. *Nucleic Acids Res.* **2000**, *28*, 235–242.
(31) Miertus, S.; Tomasi, J. *Chem. Phys.* **1982**, *65*, 239–245.
(32) Barone, V.; Cossi, M. *J. Phys. Chem. A* **1998**, *102*, 1995–2001.
(33) Cossi, M.; Rega, N.; Scalmani, G.; Barone, V. *J. Comput. Chem.* **2003**, *24*, 669–681.

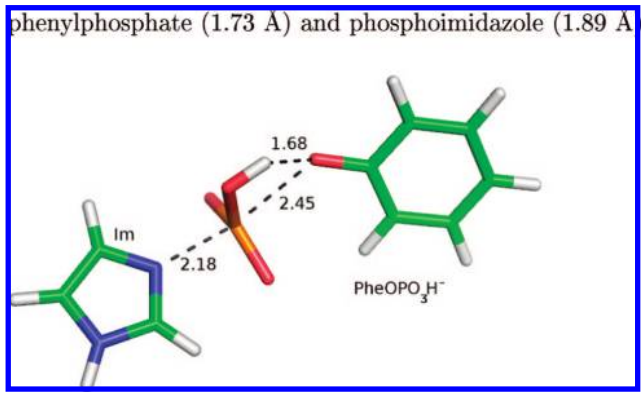

Figure 3. Optimized transition state (TS) geometry for the transfer of a phosphate group from monoanionic phenylphosphate ($PheOPO_3H^-$) to imidazole (Im) in the gas phase (Model I). Some important distances are shown in angström.

neutral His257. ONIOM calculations were carried out to obtain reactant and product states. A PES was constructed using r1 and r2 as the reaction coordinates as before to obtain an initial guess for the TS. In addition, the TS guess was also obtained using the Synchronous Transit-Guided Quasi-Newton methodology (QST2) as implemented in Gaussian03.

3. Results

3.1. Phosphoryl Transfer to Imidazole (Model I). The basic underlying chemical event in the first step of the reaction catalyzed by PAP is the transfer of a phosphate group from the phenyl group of the ligand to a nucleophilic His. This event was studied with Model I in which a monoanionic phosphate group is transferred from phenylphosphate to imidazole (as a model for His12) yielding a phenolate ion and an imidazole phosphate. The 6-31+G(d) optimized transition state is shown in Figure 3. The found TS is indeed a saddle point, as confirmed by the energy surface mapped in the immediate vicinity of it. All the absolute energies are presented in Table S1 of the Supporting Information. The distance between the phenolate oxygen and phosphate P atoms is 2.45 Å, and the $P-N_{\varepsilon 2}$ distance is 2.18 Å. It is observed that there is a little bond formation to the nucleophile when compared to the respective gas phase geometries of phenylphosphate (1.73 Å) and phosphoimidazole (1.89 Å).

The three oxygen atoms of $HPO3^-$ occupy equatorial positions with respect to P, at distances of 1.491, 1.498, and 1.625 Å (the latter refers to the oxygen with a H attached). For a relatively weak nucleophile, such as imidazole, the phosphate transfer occurs with the phosphate hydrogen atom still attached to the phosphate moiety; the O−H distance is 1.00 Å. Given that this hydrogen atom is oriented toward the leaving group (the distance between O of phenolate and H on planar metaphosphate is 1.68 Å) suggests that there is not enough charge buildup on the phenolate oxygen in the transition state to pick up the phosphate hydrogen. The Mulliken population analysis shows a charge of −0.8178.

The activation barrier for this reaction is 37.86 kcal mol^{-1} and is not greatly affected by the presence of a continuum solvent to model solvation effects (see Figure 4). As the dianionic phosphoimidazole was found to be unstable in the gas phase, the transfer of a dianionic phosphate group could not be studied.

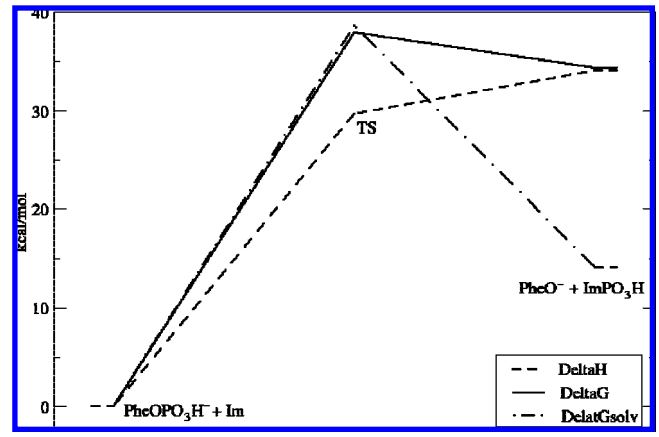

Figure 4. Energetics for the transfer of a phosphate group from monoanionic phenylphosphate ($PheOPO_3H^-$) to imidazole (Im). Change in enthalpy (ΔH) and free energies with (ΔG_{solv}) and without (ΔG) continuum solvation, of the reactants, are shown.

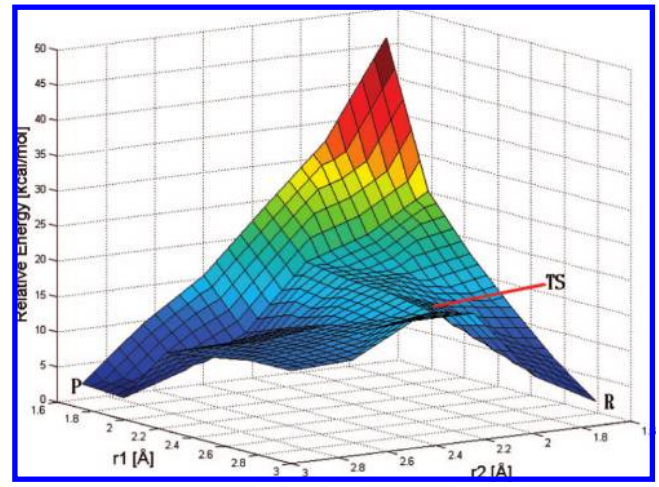

Figure 5. Potential energy surface for the reaction coordinates r1 and r2 (in Å) in the case of Model II. The symbols R, P, and TS correspond to reactant, product, and transition state structures, respectively.

3.2. Reference Reaction with Guanidium Ions (Models II and III). The most important event in enzyme-mediated catalysis involves the binding of the substrate such that in the complex the catalytic groups of the active enzyme are correctly positioned with respect to the substrate in order to commence the reaction. The binding energy is partially used to reduce the considerable contribution of the activation entropy to the total activation energy.

For PAP, it has been proposed that three nearby arginines (Arg11, Arg15, and Arg79) are important for binding of the phosphorylated ligand.[12,15] Any mutation which leads to a charge modulation in the active site abrogates the enzyme's activity. To understand the effects of these arginines and to ascertain the chosen reaction coordinates in subsequent calculations, Model II was employed, which includes three guanidium ions (to emulate arginines). In our previous study, it was observed that there is a sharing of the phosphate hydrogen (on the ligand) between the ligand itself and Asp258.[9] In the preliminary gas phase optimizations, an immediate hopping of this proton to Asp258 was observed. For this reason, Asp258 was modeled as acetic acid (and not an acetate) in the model.

Figure 5 shows the shape of the potential energy surface, with the two minima corresponding to the locations of reactants

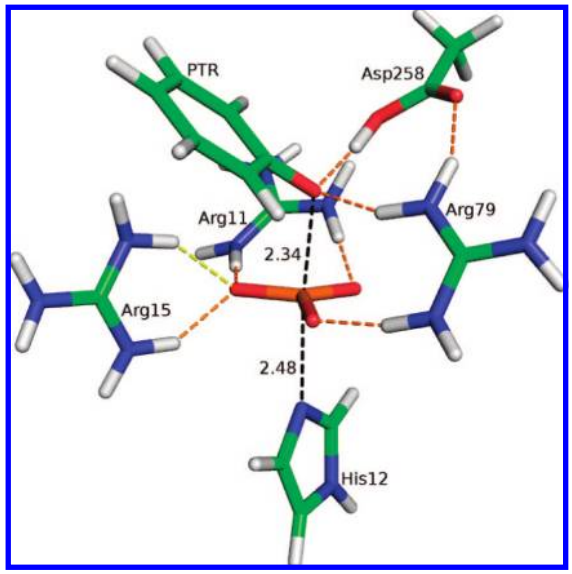

Figure 6. Optimized transition state structure for the Model II. The r1 and r2 distances (black dotted lines) are shown in angströms. Hydrogen bonds are shown in orange.

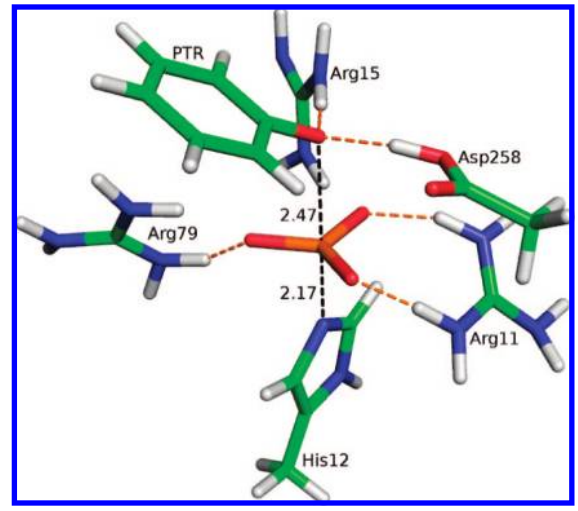

Figure 7. Optimized transition state geometry for the Model III. The r1 and r2 distances (black dotted lines) are shown in angströms. Hydrogen bonds are show in orange.

and products. The shortest path connecting the two minima goes through a small barrier in the region where the transition state (TS) would lie. The species closest to the barrier (about 17.8 kcal mol^{-1}), at r1 = 2.50 Å and r2 = 2.25 Å, was optimized, and the resulting TS (shown in Figure 6) has r1 = 2.48 Å and r2 = 2.34 Å. Numerous hydrogen bonds between the arginines and the planar PO_3^{2-} group were observed in the TS, suggesting that the arginines' role is to stabilize the TS. Arg79 moved closer to Asp258 to donate a hydrogen bond to $O_{\delta 2}$ of Asp258. Additionally, Asp258 can be seen to move closer to the phenolic oxygen O_1. The $H_{\delta 2}$ of Asp258 is seen oriented toward the O_1 of the leaving group. The distance between the O_1 of phenolate and the $H_{\delta 2}$ of Asp258 is 1.57 Å, and the $O_1-H_{\delta 2}-O_{\delta 2}$ angle is about 172°. There is a slight increase in the $O_{\delta 2}-H_{\delta 2}$ bond length ($O_{\delta 2}-H_{\delta 2}$ distance is 1.04 Å) in the TS with respect to the reactants (1.00 Å). The distance between P and O_1 (r2) is smaller (2.34 Å) with respect to Model 1 (Figure 3), and consequently the $P-N_{\varepsilon 2}$ distance (r1) is larger (2.48 Å).

Model III is virtually identical to Model II, except that a number of atoms are restrained to their respective positions as they would have in the active site. The TS obtained for this model is shown in Figure 7. The striking difference between this TS and the one obtained for Model II (Figure 6) is the r1 and r2 distances, which are now 2.17 and 2.47 Å. In addition, Arg79 now remains close to the orientation that it had in the steepest descent minimized structure and remains hydrogen bonded to the phosphate group. Another notable difference is that in Model II Arg15 was hydrogen bonded to two of the three equatorial oxygens of planar phosphate intermediate but is now hydrogen bonded to only one of them. And it is also hydrogen bonded to the leaving group oxygen (O_1).

The distance between H_{11} of Arg15 to O_1 of phenolate is decreased to 1.57 Å in the TS from 3.52 Å in the reactants' state (data not shown) and is accompanied with a slight increase in the distance between N2 and H22 of Arg15 to 1.09 Å up from 1.04 Å. There is a negligible change in the distance between $O_{\delta 2}$ and $H_{\delta 2}$ of Asp258, from 1.01 Å to 0.99 Å. The calculated energy barrier was very high, about 35.3 kcal mol^{-1}, which is 1.8 times as high in comparison to Model II. This high energy barrier could be due to two reasons. First, the arginines have long flexible sidechains that could respond to the changes in the position of the phosphate when it is being transferred from the substrate to His12. This aspect is lost when the arginines are constrained. To model this possible effect, ONIOM calculations were carried out (see below) which could allow for enough freedom of the side chains. Second, in the active site there is also a second nearby histidine (His257) whose exact role has not yet been identified. All the subsequent models (Models IV to VI) include the His257 residue.

3.3. Role of His257 (Model IV). In the TS of Model III (Figure 7), the phenolate O_1 is much closer to H_{11} of Arg15. We considered the proposition that His257 could affect the positioning of the ligand in the active site. To further investigate this hypothesis, the models were expanded to include His257. This histidine is generally considered to be positively charged,[20] and we have also kept the same protonation state, as in our previous studies.[9] As mentioned in the Methods section, a 15 Å sphere (centered around phosphate atom of the ligand) was taken along with waters for preliminary optimizations using ONIOM. The three arginines (Arg11, Arg15, Arg79), the nucleophilic His12, His257, Asp258, and the ligand jointly form the quantum motif, while the rest of the protein was treated at the MM level. Similar to the previous models, the r1 and r2 distances were restrained to 3.40 and 1.75 Å, respectively, to describe reactants in the ONIOM optimizations. The initial guess for the TS corresponded to the TS of Model II. The so-constructed Model IV was optimized using the ONIOM scheme. After these initial optimizations, the QM motif was excised from the system and subsequently employed for higher level DFT calculations to verify the TS. The resulting TS structure is shown in Figure 8.

There are a number of notable differences between the TS of Model IV and the one obtained for Model III (Figure 7). First, the barrier is substantially decreased from 35.3 kcal mol^{-1} to 26.6 kcal mol^{-1}. Second, the distance between P of the ligand and O_1 of phenolate is decreased from 2.47 to 2.30 Å, and the distance between $N_{\varepsilon 2}$ of His12 and P of the ligand changed from 2.17 Å to 2.25 Å. Third, the distance between H_{11} of Arg15 and O_1 of phenolate increased (1.75 Å), suggesting that there is an interaction between the ligand and His257, pulling the phenolate ion away from Arg15. The bond lengths between N2 of Arg15 and H_{11} of Arg15 (1.05 Å) and $O_{\delta 2}$ of Asp258 and

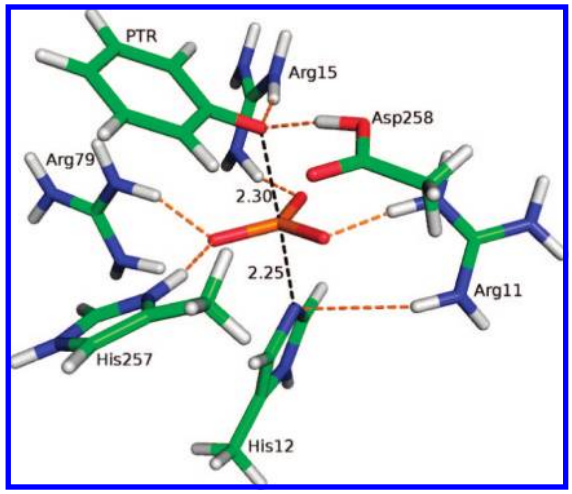

Figure 8. Optimized transition state geometry for Model IV. The r1 and r2 distances (black dotted lines) are shown in angströms. Hydrogen bonds are shown in orange.

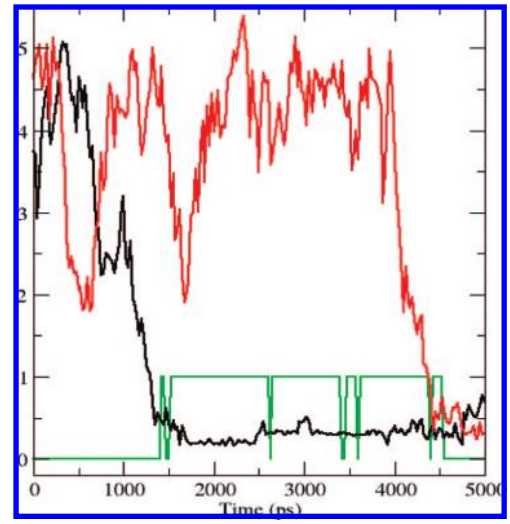

Figure 9. Minimum distance in nanometers between one of the hydrogens of the two waters (Wat1 in red and Wat2 in black) in the active site and bridging oxygen (O_1) of PTR during the course of a 5 ns MD simulation. The green line represents the number of hydrogen bonds between $H_{\delta 2}$ of Asp258 and O_w of Wat1.

$H_{\delta 2}$ of Asp258 (1.00 Å) are the same as those in the reactants. Finally, no change in the distance between $O_{\delta 2}$ of Asp258 and $H_{\delta 2}$ of Asp258 is observed, suggesting that a possible transfer of the $H_{\delta 2}$ proton of Asp258 to O_1 of phenolate may occur later in the course of the reaction. The three arginines are still involved in donating one hydrogen bond each to one of the three oxygens of the planar metaphosphate, thus stabilizing the TS.

3.4. Role of Water (Model V). It has been demonstrated that there is an early transfer of a proton from a nearby Asp to the leaving group in the low molecular weight phosphatase.[11,34] It has been argued that Asp258 could have a similar function in the active site of PAP.[18] On the other hand, there are also arguments against the role of Asp258 as a general acid in the formation of the phosphohistidine intermediate.[20] These arguments were based on the crystal structure of PAP, where Asp258 is seen to be relatively far away from the ligand, but in close proximity to Arg11. Besides, there is also evidence for the possibility, based upon studies on epoxide hydrolase, that proton transfer could be facilitated by a water bridge.[35]

It is known that, for the second step (the hydrolysis of phosphoimidazole) to proceed, there is an absolute requirement of water being in the active site and close to Asp258.[20] Water would enter the active site after the leaving group has diffused out of the active site, making the second step in fact rate limiting for the overall reaction. But an interesting question is whether the water can be found while the ligand is still in the active site. To confirm the possible presence of a water molecule, a series of MD simulations were carried out. These simulations clearly identify a water molecule being held in the right position by Asp258, shown in Figure 9, as would be required to possibly facilitate a proton transfer from Asp258 to the leaving group via the catalytic water. The water is also seen to be intermittently hydrogen bonded to Arg15. This observation assigns a possible dual role to Arg15, to stabilize the transition state and to position a water molecule for a proton transfer step. Possibly this dual role is also played by Arg15 in the hydrolysis of the phosphoenzyme intermediate where it participates in orienting a water molecule for a nucleophilic attack.

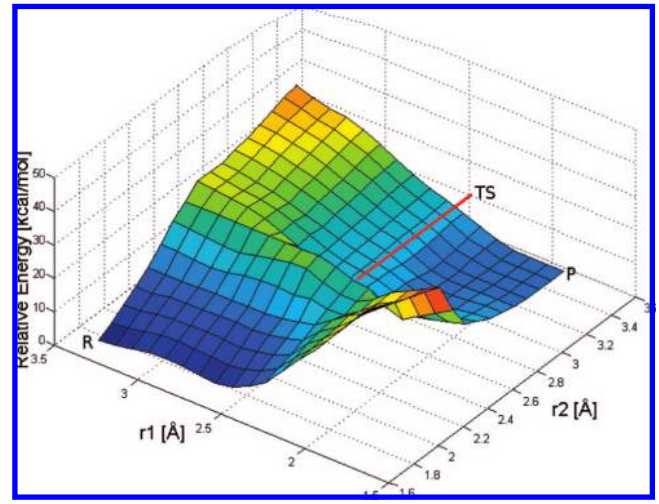

Figure 10. Potential energy surface for the reaction coordinates r1 and r2 (in Å) from the ONIOM optimizations. Only QM energies are plotted. The symbols R, P, and TS correspond to reactant, product, and transition state structures.

A structure was selected from one of the frames of the MD simulation. The same procedure of a low level ONIOM optimization was repeated, where the quantum motif now included the catalytic water. A PES scan was carried out as well, using the two distances r1 and r2, as explained in the Methods section. Figure 10 shows the resulting plot. The structure near the peak (r1 = 2.25 Å, r2 = 2.45 Å) was considered as a initial guess for high level optimizations. The barrier for the ONIOM calculation at this point was 18.2 kcal mol^{-1}.

The QM subsystem was extracted from the ONIOM system for subsequent TS optimization at a higher level. The resulting TS structure is shown in Figure 11. The barrier in this case was found to be 24.6 kcal mol^{-1}. Unexpectedly, there were only marginal differences in the r1 and r2 distances with respect

(34) Asthagiri, D.; Dillet, V.; Liu, T.; Noodleman, L.; van Etten, R. L.; Bashford, D. *J. Am. Chem. Soc.* **2002**, *124*, 10225–10235.
(35) De Vivo, M.; Ensing, B.; Klein, M. L. *J. Am. Chem. Soc.* **2005**, *127*, 11226–11227.
(36) Allen, K. N.; Dunaway-Mariano, D. *Trends Biochem. Sci.* **2004**, *29*, 495–503.

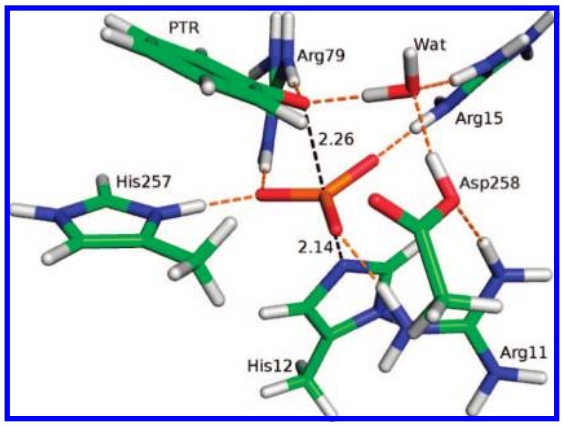

Figure 11. Optimized transition state geometry for Model V. The r1 and r2 distances (black dotted lines) are shown in angströms. Hydrogen bonds are shown in orange.

to the TS of Model IV. The catalytic water is oriented such that one of its hydrogen atoms points to O_1 of phenolate and one of the oxygen atoms of the water molecules forms hydrogen bonds to H_{11} of Arg15 and $H_{\delta 2}$ of Asp258. The O_W-H_W bond length in the water molecule is slightly increased to 1.03 Å, and the $O_W-H_W-O_1$ angle is 177.96°. Thus it appears that there is a chance that a proton from Asp258 could be transferred to O_1 of phenolate, but the actual event was not observed in the optimized TS.

3.5. Positive versus Neutral His257 (Model VI). From the TS of Model V, it appeared that there was not enough charge buildup on the O_1 atom of phenolate for it to accept a proton from a water molecule, which appeared to be very well positioned for donating one of its hydrogens. Based on the proximity of His257 to the leaving group and the lack of any concrete experimental evidence for it to be positively charged, the previous calculations were repeated but now with a neutral His257. The MD simulations were also repeated with a neutral His257. The change had no significant effect on the entry and further favorable positioning of the water molecule in the active site (data not shown). The orientation of water and its hydrogen bonding pattern appeared to be same as in the case of positive His257.

A partial scan using the r1 and r2 distances employing high level DFT was carried out to find an initial guess for subsequent TS optimizations. Simultaneously, we also obtained a guess from the QST2 routine as implemented in Gaussian 03. Both guesses independently yielded the same transition state structure with a barrier of 23.5 kcal mol^{-1} (this amounts to a 1.1 kcal mol^{-1} lower barrier as compared to positive His257). The TS structure is shown in Figure 12. The distance between P of phosphate and O_1 of phenolate is 2.40 Å. The distance between $N_{\varepsilon 2}$ of His12 and P of phosphate is 2.62 Å. There is a complete transfer of the proton from Asp258 via the catalytic water to the leaving phenolate in the TS. This suggests the importance of a neutral His257 in promoting the basicity of the leaving group. The $H_{\delta 2}$ of Asp258 restored the catalytic water resulting in negatively charged Asp258, an absolute requirement for the reaction to move into the second step involving phosphohistidine hydrolysis.

4. Discussion

A vast majority of cellular activities requires (de)phosphorylation reactions. Enzymatic dephosphorylation depends on a phosphorylated enzyme intermediate, the formation of which

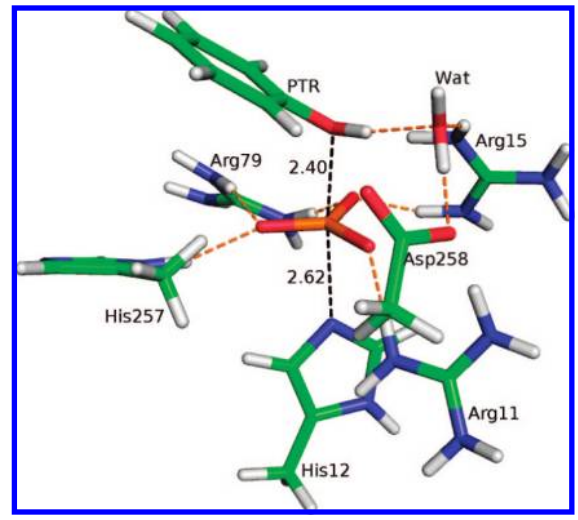

Figure 12. Optimized transition state geometry for Model VI. The r1 and r2 distances (black dotted lines) are shown in angströms. Hydrogen bonds are shown in orange.

involves a nucleophilic attack by a residue of the enzyme on the phosphate of the respective ligand, and a suitable base to donate a proton to the leaving group. The histidine acid phosphatases form a distinct class of enzymes sharing a common active site structure. These enzymes are characterized by the presence of a conserved RHGXRXP motif, which contains the nucleophilic His. The motif is located at the bottom of the active site cleft surrounded by positively charged arginines on one side, where it is secluded from water.[12,14,15] This results in a stabilization of the deprotonated state of His, effectively lowering its pK_a, such that it becomes highly suitable to act as a nucleophile for the attack.[37] Consequently, histidine acid phosphatases display an acidic pH optimum.[38] The His-Asp motif lines the other side of the cleft opposite to the arginines such that the area for ligand binding is in between this motif and the arginines. The crystal structures of *E. coli* phytase,[38] *E.coli* glucose-1-phosphatase,[37] and PAP[20] show that the phosphate moiety is bound in the active site cleft with an identical pattern of hydrogen bonding irrespective of the nature of the ligand. Thus it seems likely that they also share the same general reaction mechanism, which emphasizes the importance of this work.

This paper specifically deals with PAP (prostatic acid phosphatase). The RHGXRXP motif contains His12 serving as the nucleophile.[12,14,15] Asp258 of the His-Asp motif has been suggested by some authors to be involved as a base in this first step.[18,19] This suggestion was however disputed by others.[20] The role of Asp258 is still uncertain and is not clearly understood. We agree with Ortlund et al.[20] that, at the enzyme's optimum pH, the substrate would enter the active site carrying a hydrogen, while Asp258 is deprotonated. However, this work has demonstrated that Asp258 can be protonated in the course of the binding step. When the phosphate monoanion was considered in the active site, preliminary quantum chemical optimizations invariably showed that the phosphate proton transferred to Asp258. Also, from our earlier MD simulations of the PAP−ligand complex using different protonation states,[9]

(37) Lee, D. C.; Cottrill, M. A.; Forsberg, C. W.; Jia, Z. *J. Biol. Chem.* **2003**, *278*, 31412–31418.
(38) Lim, D.; Golovan, S.; Forsberg, C. W.; Jia, Z. *Nat. Struct. Biol.* **2000**, *7*, 108–113.

Table 1. Contributions to the Transition State Stabilization or Destabilization (in kcal mol^{-1}) Based on B3LYP/6-31+G(d) Calculations

no.	ΔE	contributed by
Model I and II	>10	unrestrained arginines
Model I and III	−5.6	restrained arginines
Model III and IV	8.7	positive His257
Model IV and V	2.0	catalytic water
Model V and VI	1.1	neutral His257

it was observed that there was a tendency for the system to share the phosphate hydrogen atom between the ligand and Asp258. In addition, with a fully deprotonated Asp258 and the ligand placed in the active site as a monoanion, the complex was becoming increasingly unstable as the ligand was pushed out of the active site due to unfavorable interactions. Because of these observations, it was concluded that, upon binding, the ligand phosphate would become dianionic with Asp258 becoming neutral by accepting a proton from the incoming phosphate group. With all the equatorial oxygens of phosphate hydrogen bonded to nearby arginines, the oxygen carrying the hydrogen is likely to be positioned near Asp258. To further verify this conclusion, reactant models similar to models III to VI were built with a monoanionic phosphate instead of a dianion and optimized. In all cases, including those with ONIOM, it was again observed that the proton was donated by monoanionic phosphate to Asp258 during the geometry optimizations. This occurs irrespective of the protonation state of His257. In fact, constraining the proton to remain on the phosphate resulted in a geometry that is about 13 kcal mol^{-1} higher in energy (data not shown). It appears then that a proton jump from the equatorial oxygen to Asp258 is favorable. So, we consider that the ligand would be dianionic in the active site with Asp258 being neutral.

The arginines in the active site of the enzyme stabilize the transition state through hydrogen bonds to the planar metaphosphate with each arginine donating at least one hydrogen bond to one of the equatorial oxygens. Exceptionally, in the case of Model II (where atoms were not restrained to positions according to the crystal structure of the free enzyme) there was a higher number of hydrogen bonds to the phosphate. Thus, our findings are in correspondence with the expected role of arginines in stabilizing an anionic intermediate by an amount more than 10 kcal mol^{-1} (see Table 1). The similar role of arginines has also been observed in other phosphotransfer reactions such as in the case of low molecular weight phosphatase[34] and in the crystal structure of phosphorylated β-phosphoglucomutase.[39] In PTPs, the signature motif $(H/V)C(X)_5R(S/T)$ harbors the active site arginine. This invariant arginine is important for both substrate binding and transition state stabilization.[34] PAP has two consereved arginines (Arg11 and Arg15) in the conserved motif. Arg11 is engaged in two hydrogen bonds to the ligand oxygens in quite the same way as the Arg of PTP, and hence Arg11 is similarly important for initial recognition and further binding of the substrate.

During the dephosphorylation, the observed extent of $P-O_l$ bond lysis largely depends on the model employed for a calculation. It was noted that Model III (without His257) displayed a more extensive lysis of the $P-O_l$ bond in comparison to Model IV (with His257). It is very interesting to compare the transition state (TS) of Model IV with the transition state occurring during phosphorylation catalyzed by human bisphosphoglycerate mutase (PGM), which was studied by Wang et al.[40] The TS of our structure is very similar to the one attained by the PGM enzyme, which was crystallized with AlF3 as a TS analogue. Wang's studies show that the reaction proceeds according to an S_N2 mechanism (28% associative). The distance between the nucleophile and the leaving group was 4.1 Å, while our calculations for PAP resulted in a distance of 4.55 Å.

As already alluded to above, Asp258 also oriented itself to possibly act as the hydrogen donor to the leaving group. When the various atoms were restrained to their respective positions as expected in the active site (Model III), the orientation of Asp258 did not appear to facilitate the early donation of a proton to the leaving group. Although the inclusion of a positively charged His257 in the model (Model IV) resulted in a decrease of the energy barrier, a proton transfer to the leaving group was still not observed.

When the structure of PAP is viewed in a surface representation, one clearly observes a large channel that spans through the enzyme from its surface to the active site, which would allow for water molecules to freely move in and out of the active site. In our previous study on ligand binding we have shown that the ligand peptide lies on the protein's surface effectively blocking one side of the channel.[9] This would still allow water to enter the active site through the other side. The identification of water in the active site of PAP as was observed during MD simulations suggested that a water molecule possibly acts as an intermediate in the transfer. The possibility that a catalytic water is involved in the proton transfer is not unusual.[35] In PAP, the Arg15 is instrumental as a "finger", in holding this water in position and simultaneously forming a hydrogen bond with the phsophate. Similar to this, a computational study on RasGAP, an enzyme that hydrolyzes GTP, also pointed out the importance of an arginine residue in forming hydrogen bonds to the phosphate and a catalytic water as well.[41]

The results presented in this work also highlight the importance of His257. Vihko et al.[18] have shown that a mutation of His257 to Ala drastically impairs the enzyme activity. An explanation for this result was however not offered. This work shows that neutral His257 lies nearly parallel to the ring of leaving phenolate. This interaction builds up a negative charge on phenolate oxygen resulting in early protonation of the leaving group by the water molecule in the active site which slightly lowers the barrier (see Table 1). Based on the obtained results it is concluded that Asp258 is not directly involved in the protonation of the leaving group; rather the transfer of a proton from Asp258 to the leaving group is mediated by a water molecule in the active site.

There has been considerable debate in the literature about the nature of the transition state in enzymes catalyzing phosphotransfer reactions. In solution, the hydrolysis of phosphomonoesters proceed by a dissociative-like mechanism. Enzymes apparently can use either associative or dissociative mechanisms.[42] The MoreO'Ferrall−Jencks plot[43] suggests that the associative nature is defined by a decrease (formation) of the $P-O_{nuc}$ bond followed by an increase (breakage) of the $P-O_{lg}$ bond. According to this, all the observed transition states

(39) Lahiri, S. D.; Zhang, G.; Dunaway-Mariano, D.; Allen, K. N. *Science* **2003**, *299*, 2067–2071.

(40) Wang, Y.; Liu, L.; Wei, Z.; Cheng, Z.; Lin, Y.; Gong, W. *J. Biol. Chem.* **2006**, *281*, 39642–39648.

(41) Resat, H.; Straatsma, T. P.; Dixon, D. A.; Miller, J. H. *Proc. Natl. Acad. Sci. U.S.A.* **2001**, *98*, 6033–6038.

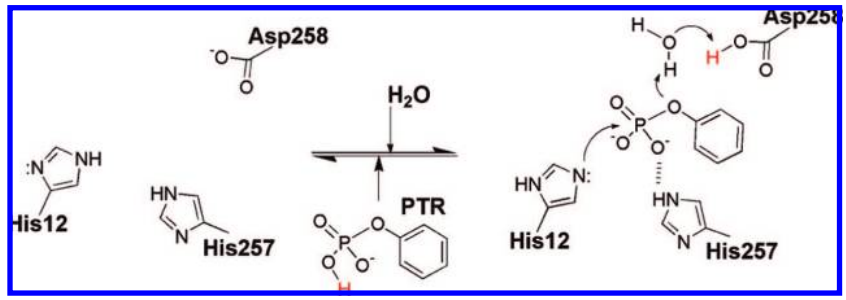

Figure 13. Proposed reaction scheme based on this work. Phenylphosphate enters the active site with a hydrogen (in red), which is immediately transferred to Asp258. His12 acts as the nucleophile. His257 is proposed to be neutral. The transfer of proton to the leaving group from Asp258 is mediated via a catalytic water.

in the present study can be assigned an associative character. The planar guanidinium group has also been considered as a requirement for a dissociative-like transition state.[42] The present work has conclusively shown for the first time that this planarity is not the only requirement for dissociative character, if at all. The TS observed for Model II is not dissociative despite nearby planar guanidium groups stabilizing the negative charges on the phosphate entity.

5. Conclusions

On the basis of the present and our previous work,[9] we propose the following mechanism for the first step of the dephosphorylation reaction catalyzed by PAP (Figure 13). The free enzyme contains a negatively charged Asp258. The ligand enters the active site with phosphate as a monoanion ($ROPO_3H^-$). The proton on the phosphate is transferred from the phosphate group to Asp258, which consequently is protonated in the course of the binding process. The phosphodianion is stabilized by the three nearby arginines. His257 is important in orienting the substrate and later for the modulation of charge on the leaving group. A water in the active site is held in position by Asp258 and Arg15. His12 acts as the nucleophile and attacks the phosphate of the ligand. With the breaking of the bond between the bridging oxygen and the phosphorus on the ligand, the bridging oxygen of the ligand extracts the proton from the active site water molecule. The generated hydroxyl ion picks up the proton on Asp258, and thus the water is regenerated. The TS is identified as being a concerted transition state with near associative character. The phosphohistidine intermediate is formed, and the leaving group diffuses out of the binding pocket.

Acknowledgment. We thank CSC (Center of Scientific Computing) in Espoo (Finland) for providing computing power. We also express our gratitude to Rickard Gail and Jie Li for their help in carrying out these calculations. TEKES (Finnish Funding Agency for Technology and Innovation) and the Department of Biochemistry of the University of Oulu are acknowledged for financial support. We also acknowledge the reviewers, for their constructive criticism has greatly improved the quality of the manuscript.

Supporting Information Available: Comparison of B3LYP/6-31+G(d) and B3LYP/6-31G(d) geometries, table of PES surface for model I, absolute energies of stationary points, Cartesian coordinates for the transition state along with frequencies and transition vectors. Complete refs 21 and 22. This material is available free of charge via the Internet at http://pubs.acs.org.

JA710047A

(42) Fauman, E. B.; Yuvaniyama, C.; Schubert, H. L.; Stuckey, J. A.; Saper, M. A. *J. Biol. Chem.* **1996**, *271*, 18780–18788.
(43) Kamerlin, S. C. L.; Wilkie, J. *Org. Biomol. Chem.* **2007**, *5*, 2098–2108.